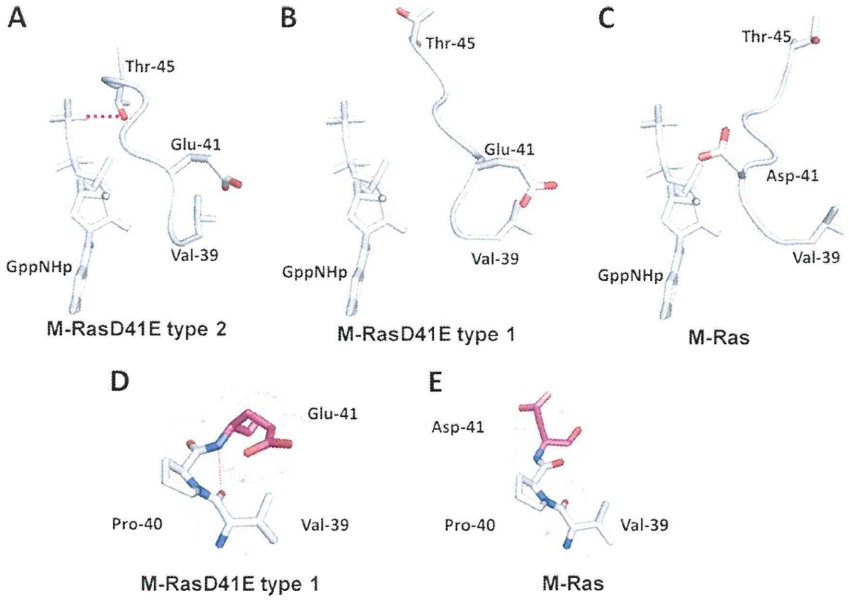

FIGURE 5. **Main chain and side chain configurations of the pre-switch I and switch I residues of M-Ras-GppNHp and M-RasD41E-GppNHp types 1 and 2.** The backbone structures of the pre-switch and switch I regions and the structure of GppNHp are shown for M-RasD41E-GppNHp type 2 (*A*), M-RasD41E-GppNHp type 1 (*B*), and M-Ras-GppNHp (*C*), on which only the side chains of Val-39, Glu/Asp-41, and Thr-45 are depicted (*red*, oxygen). The hydrogen bond between Thr-45 and the γ-phosphate in M-RasD41E-GppNHp type 2 is shown by a *red broken line*. The van der Waals distances for Val-39, Pro-40, and Glu/Asp-41 of M-RasD41E-GppNHp type 1 (*D*) and M-Ras-GppNHp (*E*) are highlighted, where a *red dotted line* represents a hydrogen bond. The models were generated by PyMOL.

GppNHp type 2, the side chain of Glu-41 is arranged face to face with that of Val-39 and pulled away from the nucleotide (Fig. 5*A*). A hydrophobic interaction of C_δ of Glu-41 with the C_γ of Val-39 appears to play a role in establishing this constellation. In contrast, Asp-41 of M-Ras-GppNHp fails to establish any interactions with Val-39 and Pro-40, leading to marked displacement of Asp-41 from Val-39 (Fig. 5*C*), which could be accounted for by the fact that the shorter side chain of Asp-41 prohibits the formation of a van der Waals contact with the side chain of Val-39 or Pro-40 (Fig. 5*E*). Intriguingly, M-RasD41E-GppNHp type 1 exhibits a constellation of Glu-41 and Val-39 very similar to that of type 2 as characterized by a flip of Glu-41 away from the nucleotide (Fig. 5*B*). The underlying mechanism could be that the longer side chain of the Glu-41 substitute restored the van der Waals interactions with the side chain of Val-39 (Fig. 5*D*).

Superimposition of the main chain and side chain structures of residues 39–45 of M-Ras-GppNHp and M-RasD41E-GppNHp type 1 (Fig. 6*A*) reveals that the inside-out flip of Glu-41 (*arrow a*) causes substantial rotational and positional changes of the backbone structure of the switch I loop and pre-switch I residues starting at Pro-40. For example, the (ϕ, ψ) dihedral angles of Pro-40 and residue 41 exhibit significant changes from (−51°, 147°) and (41°, 44°), respectively, in M-Ras-GppNHp to (−54°, −31°) and (−84°, −5°), respectively, in M-RasD41E-GppNHp type 1. These conformational changes, resulting from the D41E substitution, induce a gross regional rearrangement of the hydrogen-bonding network involving the switch I loop and pre-switch I residues: both the direct interaction of the Asp-41 side chain with the ribose and the water-mediated interaction of the main chain carbonyl group of Tyr-42 with the α-phosphate in M-Ras-GppNHp are lost and replaced by the newly formed hydrogen bond between the main chains of Glu-41 and Asp-43 in M-RasD41E-GppNHp type 1 (Fig. 6*A* and supplemental Fig. S2). Thus, the rotational and positional changes initiated at the pre-switch I residues are conveyed to the switch I loop, resulting in the positional shift of Thr-45 approaching the γ-phosphate (*arrow b*). As already discussed, this positional shift of Thr-45 is likely to facilitate the formation of a hydrogen bond with the γ-phosphate and may account for the increase of the state 2 population in M-RasD41E-GppNHp. The reason why M-RasD41E-GppNHp type 1 failed to establish Thr-45-γ-phosphate hydrogen-bonding interaction despite the adoption of the type 2-like constellation of Val-39 and Glu-41 could be accounted for by the presence of Pro-40, which exerts a rotational constraint on the backbone structure.

FIGURE 4. **^{31}P NMR spectra of the GppNHp-bound M-Ras mutants bearing H-Ras-type amino acid substitutions in the α3-helix.** *A*, the spectra were recorded using 1 mM solution of the indicated M-Ras mutant and H-Ras proteins in complex with GppNHp. α, β, and γ represent the α-, β- and γ-phosphate resonances, respectively. (*1*) and (*2*) represent the γ-phosphate resonance peaks corresponding to states 1 and 2, respectively. α_{free}, β_{free}, and γ_{free} represent the α-, β-, and γ-phosphate resonances of the free GppNHp, respectively. α-*GDP* and β-*GDP* represent the α- and β-phosphate resonances, respectively, of GDP bound to the M-Ras mutants. *B*, *bar graph* representation of state 2 populations of the M-Ras mutants in complex with GppNHp. The state 1 and state 2 peaks in the γ-phosphate resonance were fitted by Lorentz curves (*blue lines* in *A*), and the state 2 population was calculated as [state 2]/([state 1]+[state 2]), where [state 1] and [state 2] represent the relative concentrations obtained as the integrals of the corresponding peaks. *Error bars*, S.D. derived from the Lorentz curve fitting. The data of H-Ras-GppNHp and M-RasP40D/D41E/L51R/F74Y/E79D-GppNHp were adopted from our previous reports (18, 21).

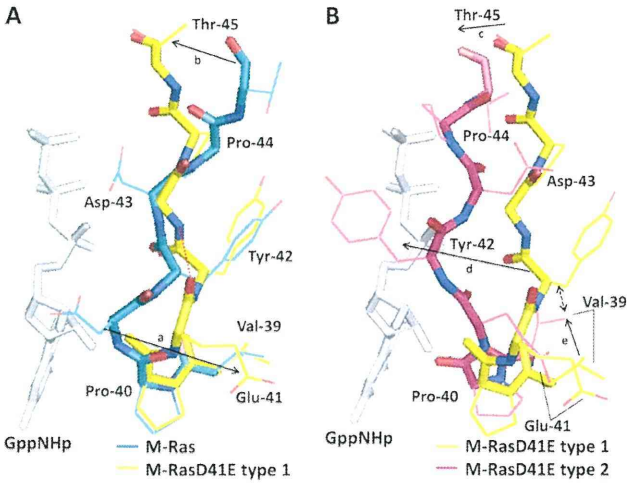

FIGURE 6. **Comparison of the structures of the pre-switch I and switch I regions among M-Ras-GppNHp and M-RasD41E-GppNHp types 1 and 2.** Shown are superimpositions of the structures of the residues 39–45 of M-Ras-GppNHp (*light blue*) and M-RasD41E-GppNHp type 1 (*yellow*) (*A*) and M-RasD41E-GppNHp type 1 (*yellow*) and type 2 (*pink*) (*B*) are shown. The structure of GppNHp (*white*) is excerpted from the model of M-RasD41E-GppNHp type 1. Main chains and side chains are shown by *thick* and *thin bars*, respectively, on which oxygen and nitrogen atoms are shown by *red* and *blue colors*, respectively. *Arrows a* and *b* in *A* represent the conformational changes of Glu-41 and Thr-45, respectively, whereas *arrows c, d,* and *e* in *B* represent those of Thr-45, Tyr-42, and Val-39, respectively. A *red dotted line* in *A* shows the hydrogen bond between the main chains of Glu-41 and Asp-43. A *bidirectional broken arrow* represents the collision of the side chain of Tyr-42 with that of Val-39. The models were generated as described in the legend to Fig. 2.

Determination of both the state 1 and state 2 structures from M-RasD41E-GppNHp enables us to analyze the state transition mechanisms through comparison of the two structures. Superimposition of residues 39–45 of type 1 and type 2 (Fig. 6*B*) reveals drastic changes in the main chain and side chain structures of the switch I loop and pre-switch I residues, resulting in establishment of the Thr-45-γ-phosphate hydrogen-bonding interaction in type 2 (*arrow c*). Type 2, but not type 1, forms both direct and water-mediated hydrogen bonds between Pro-40 and the ribose, and a water-mediated hydrogen bond between Glu-41 and the α-phosphate (Fig. 2 and supplemental Fig. S2). Above all, Tyr-42 exhibits the most drastic positional and rotational change toward the nucleotide (*arrow d*). This is presumably caused by collision of Tyr-42 with the side chain of Val-39 (bidirectional *broken arrow*), which undergoes a positional change (*arrow e*) during the state 1 to state 2 transition.

Collectively, the results demonstrate that having Glu at residue 41 of M-Ras plays a pivotal role in the adoption of the state 2 conformation for the following two reasons. 1) The interaction of Glu-41 with the neighboring Val-39 causes a rotational change of the pre-switch I residues, leading to the switch I loop conformational change in combination with the rearrangement of the hydrogen-bonding network involving the switch I loop, pre-switch I residues, and the nucleotide. As a result, Thr-45 undergoes a positional shift approaching the γ-phosphate, facilitating the formation of a hydrogen bond with the γ-phosphate. 2) The remarkable displacement of Tyr-42 through the positional change of Val-39 brings about a drastic conformational change of the switch I loop toward the nucleotide, leading to the Thr-45-γ-phosphate hydrogen bond formation (see Fig. 2*A*). On the contrary, having Asp at residue 41 as in the case of M-Ras-GppNHp totally abolishes the corresponding interactions and facilitates the adoption of state 1.

State-specific Constellations of the Pre-switch I Residues Conserved Among M-Ras, H-Ras, and Their Mutants—The critical role of residue 41 in the state transition of M-Ras-GppNHp and M-RasD41E-GppNHp lead us to examine intramolecular interactions involving pre-switch I residues in H-Ras-GppNHp, H-RasT35S-GppNHp, and M-RasP40D/D41E/L51R-GppNHp. The configuration of the residues 31/41 (H-Ras/M-Ras) showed a clear difference between state 1 and state 2 conformers (Fig. 7). In state 2 conformers, H-Ras-GppNHp and M-RasP40D/D41E/L51R-GppNHp, their Glu-31/41 residues establish interactions with neighboring residues 29/39 and/or 30/40, leading to adoption of a constellation of residues 29/39 and 31/41, which is equivalent to that of M-RasD41E-GppNHp type 2 (Figs. 5*A* and 7*A*). However, the mode of interactions is different among the three proteins. In H-Ras-GppNHp, the side chain carboxyl group of Glu-31 forms a water-mediated hydrogen bond with the main chain amide of Asp-30, which is presumably assisted by a van der Waals contact of the C_δ of Glu-31 with the C_γ of Val-29 (Fig. 7*C*). In the case of M-RasP40D/D41E/L51R-GppNHp (PDB code 3KKO, chain A), both the main chain and side chain of Asp-40 formed water-mediated hydrogen bonds with the side chain of Glu-41 (data not shown). As already discussed, in the case of M-RasD41E-GppNHp type 2, a hydrophobic interaction of C_δ of Glu-41 with the C_γ of Val-39 appears to be involved. In contrast, Glu-31 of the state 1 conformer, H-RasT35S-GppNHp form 2, fails to establish any interactions with Val-29 and Asp-30, leading to marked displacement of Glu-31 from Val-29 as observed in M-RasGppNHp (Figs. 5*C* and 7*B*), whose shorter side chain of Asp-41 prohibits interaction with Val-39 or Pro-40 as already discussed (Fig. 5*E*). In this case, the loss of the Glu-31—Val-29 interaction presumably occurs by the marked deviation of the switch I loop following the loss of the Ser-35-γ-phosphate interaction. As already pointed out, M-RasD41E-GppNHp type 1 (state 1) represents an exceptional case; it exhibits a constellation of Glu-41 and Val-39 very similar to that of the state 2 conformers (Fig. 5*B*), which can be explained that the longer side chain of the Glu-41 substitute restores the van der Waals interactions with the side chain of Val-39 (Fig. 5*D*). These results collectively indicate that the critical role of the Glu-31/41—Val-29/39 interaction in adoption of the state 2 conformation is conserved between M-Ras and H-Ras. It is also supported by the observation that H-RasV29G-GppNHp exhibits a vast increase in the state 1 population as assessed from its ^{31}P NMR spectrum (30).

The study on M-RasD41E-GppNHp types 1 and 2 also has indicated the importance of the displacement of Tyr-42 through the positional change of Val-39 in the conformational change of Thr-45 leading to the establishment of its interaction with the γ-phosphate. Comparison of the structures of the pre-switch I and switch I regions between H-RasT35S-GppNHp form 2 and H-Ras-GppNHp shows the existence of a similar displacement of Tyr-32 toward the nucleotide in H-Ras-GppNHp, which is presumably caused by the positional change of Val-29 (supplemental Fig. S6). Thus, this mechanism may also be shared between M-Ras and H-Ras.

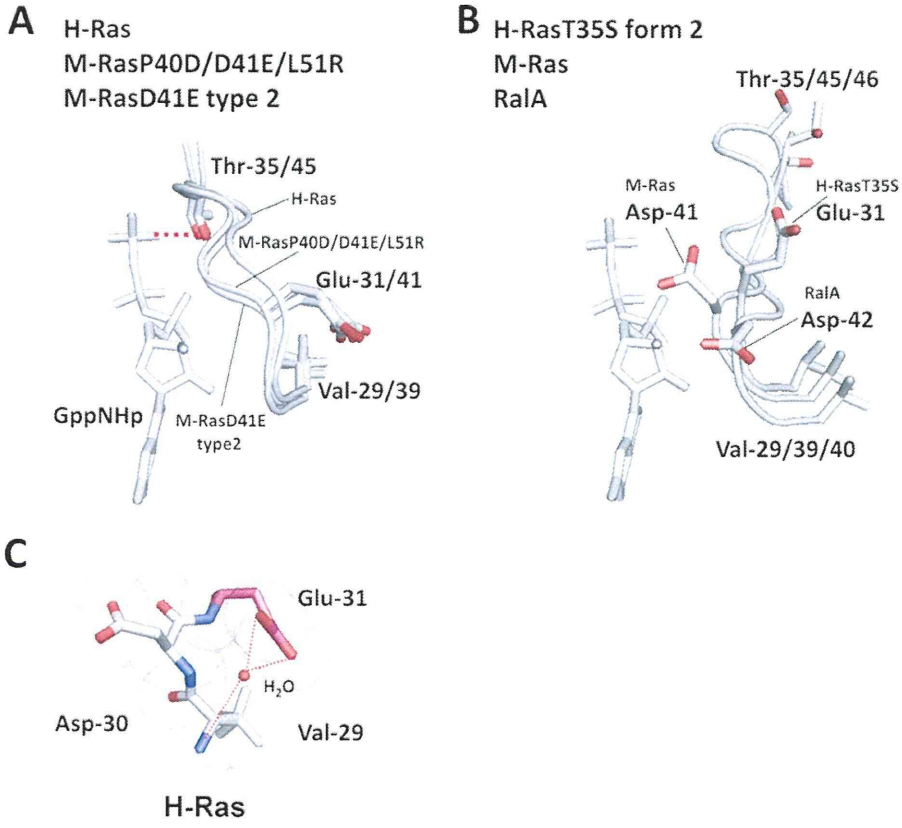

FIGURE 7. **Comparison of the structures of the pre-switch I and switch I regions among M-Ras, H-Ras, RalA, and their mutants.** Shown are superimpositions of the structures of the residues 29–35/39–45/40–46 (H-Ras/M-Ras/RalA) of the state 2 conformers, M-RasD41E-GppNHp type 2, M-RasP40D/D41E/L51R-GppNHp, and H-Ras-GppNHp (*A*), and of the state 1 conformers, M-Ras-GppNHp, H-RasT35S-GppNHp form 2, and RalA-GppNHp (*B*). The structures of GppNHp are excerpted from the models of H-Ras-GppNHp (*A*) and M-Ras-GppNHp (*B*). The side chains of residues 29/39/40, 31/41/42, and 35/45/46 (H-Ras/M-Ras/RalA) are highlighted with the stick model (*red*, oxygen). The hydrogen bond between Thr-35 and the γ-phosphate in H-Ras is shown by a *red broken line*. The models were generated as described in the legend to Fig. 1. *C*, van der Waals distances for Val-29, Asp-30, and Glu-31 of H-Ras-GppNHp are highlighted. *Red dotted lines* represent hydrogen bonds. The models were generated by the program PyMOL.

Conservation of the Roles of the Novel Intramolecular Interactions in a More Distantly Related Ras Family Member, RalA—Conservation of the critical roles of the two interactions, around the pre-switch I residues and between switch II and the α3-helix, in the state transition of M-Ras and H-Ras leads us to test whether a similar mechanism is working in more distantly related members of Ras family small GTPases. To this end, we focus on RalA, whose switch I residues are poorly conserved (supplemental Fig. S1), because it is the only Ras family member whose state 1 crystal structure has been determined other than M-Ras, H-Ras, and their mutants (31). RalA-GppNHp mainly adopts state 1 in solution with a state 1 population of 53 ± 7% (12). The crystal structure of RalA-GppNHp corresponds to state 1 judging from the loss of the interaction of Thr-46 (corresponding to Thr-35/45 of H-Ras/M-Ras) with the γ-phosphate (31) and its backbone structure of switch I superimposes very well with that of M-Ras-GppNHp (data not shown) despite the existence of non-conserved residues, Glu-44, Lys-47, and Ala-48 (corresponding to Asp-33/43, Ile-36/46, and Glu-47 of H-Ras/M-Ras) (see supplemental Fig. S1). In RalA-GppNHp, Asp-42, equivalent to Asp-41 in M-Ras, fails to interact with Val-40, equivalent to Val-39 in M-Ras, adopting a constellation of the pre-switch I residues analogous to those of state 1 structures of M-Ras and H-Ras (Fig. 7*B*).

On the other hand, RalA-GppNHp retains the hydrogen-bonding interaction of Gly-71 (corresponding to Gly-60/70 of H-Ras/M-Ras) with the γ-phosphate (31) (supplemental Fig. S7). In RalA-GppNHp, Gln-110 in the α3-helix, equivalent to Gln-99 of H-Ras, formed hydrogen bonds with Ile-78 and Asp-80 in switch II, like the case of H-Ras-GppNHp, whereas Phe-107, equivalent to Phe-106 of M-Ras, fails to interact with switch II residues, such as M-RasD41E-GppNHp type 1. This is consistent with our notion that the higher density or the proper arrangement of the hydrogen-bonding network between switch II and the α3-helix facilitates the adoption of state 2, resulting in the higher state 2 population. These results suggest that RalA shares a similar mechanism of state transition with M-Ras and H-Ras.

In conclusion, our study has demonstrated the critical roles of the two novel intramolecular interactions in the state 1 to state 2 transition; one around the pre-switch I residues and the other between switch II and the α3-helix, which appear to facilitate the formation of hydrogen bonds of Thr-35/45 (H-Ras/M-Ras) in switch I and Gly-60/70 in switch II with the γ-phosphate of GTP, respectively. Although it is evident that the four interactions are intimately related with one another, the sequence of these various events cannot be determined from the present study, which deals with static structures. This mechanism of

state transition seems to be conserved among M-Ras, H-Ras, and more distantly related RalA. Thus, the amino acid sequence diversity of the residues involved in the relevant interactions seems to be responsible for determination of the intrinsic state distribution of Ras family small GTPases. Our work also suggests that the P-loop may have a role in the state transition via interaction with the α3-helix. This is supported at least in part by the observation that P-loop mutants of H-Ras, such as H-RasG12V and H-RasG12D, showed an increase in the state 1 population in their GppNHp-bound forms (10, 30). The α3-helix and P-loop were thought to be rather immobile from crystallographic studies. However, the backbone amide ^{15}N spin relaxation rcCPMG measurements by O'Connor *et al.* (32) suggested that they exhibit a significant mobility upon state transition, which is further supported by our latest study[4] of ^{15}N relaxation times and heteronuclear nuclear Overhauser effects of H-RasT35S-GppNHp. As already proposed (21), the various events relevant to the state transition could be targeted for development of Ras inhibitors, *i.e.* inhibition of the state 1 to state 2 transition leads to inactivation of the Ras function.

Acknowledgments—The synchrotron radiation experiments were performed at BL38B1 and BL41XU in SPring-8 with the approval of the Japan Synchrotron Radiation Research Institute (JASRI) (Proposal number 2009B1117). We thank Kazuya Hasegawa, Nobutaka Shimizu, Seiki Baba, Nobuhiro Mizuno, and Masatomo Makino of JASRI/SPring-8 for data collection in the SPring-8 and for technical advice. We thank Tomoko Inoue and Shinya Ichikawa for excellent technical assistance.

REFERENCES

1. Takai, Y., Sasaki, T., and Matozaki, T. (2001) *Physiol. Rev.* **81,** 153–208
2. Downward, J. (2003) *Nat. Rev. Cancer* **3,** 11–22
3. Karnoub, A. E., and Weinberg, R. A. (2008) *Nat. Rev. Mol. Cell Biol.* **9,** 517–531
4. Corbett, K. D., and Alber, T. (2001) *Trends Biochem. Sci.* **26,** 710–716
5. Vetter, I. R., and Wittinghofer, A. (2001) *Science* **294,** 1299–1304
6. Nassar, N., Horn, G., Herrmann, C., Scherer, A., McCormick, F., and Wittinghofer, A. (1995) *Nature* **375,** 554–560
7. Geyer, M., Herrmann, C., Wohlgemuth, S., Wittinghofer, A., and Kalbitzer, H. R. (1997) *Nat. Struct. Biol.* **4,** 694–699
8. Huang, L., Hofer, F., Martin, G. S., and Kim, S. H. (1998) *Nat. Struct. Biol.* **5,** 422–426
9. Pacold, M. E., Suire, S., Perisic, O., Lara-Gonzalez, S., Davis, C. T., Walker, E. H., Hawkins, P. T., Stephens, L., Eccleston, J. F., and Williams, R. L. (2000) *Cell* **103,** 931–943
10. Geyer, M., Schweins, T., Herrmann, C., Prisner, T., Wittinghofer, A., and Kalbitzer, H. R. (1996) *Biochemistry* **35,** 10308–10320
11. Spoerner, M., Nuehs, A., Herrmann, C., Steiner, G., and Kalbitzer, H. R. (2007) *FEBS J.* **274,** 1419–1433
12. Liao, J., Shima, F., Araki, M., Ye, M., Muraoka, S., Sugimoto, T., Kawamura, M., Yamamoto, N., Tamura, A., and Kataoka, T. (2008) *Biochem. Biophys. Res. Commun.* **369,** 327–332
13. Fenwick, R. B., Prasannan, S., Campbell, L. J., Nietlispach, D., Evetts, K. A., Camonis, J., Mott, H. R., and Owen, D. (2009) *Biochemistry* **48,** 2192–2206
14. Quilliam, L. A., Castro, A. F., Rogers-Graham, K. S., Martin, C. B., Der, C. J., and Bi, C. (1999) *J. Biol. Chem.* **274,** 23850–23857
15. Rodriguez-Viciana, P., Sabatier, C., and McCormick, F. (2004) *Mol. Cell. Biol.* **24,** 4943–4954
16. Pai, E. F., Krengel, U., Petsko, G. A., Goody, R. S., Kabsch, W., and Wittinghofer, A. (1990) *EMBO J.* **9,** 2351–2359
17. Scheidig, A. J., Burmester, C., and Goody, R. S. (1999) *Structure* **7,** 1311–1324
18. Ye, M., Shima, F., Muraoka, S., Liao, J., Okamoto, H., Yamamoto, M., Tamura, A., Yagi, N., Ueki, T., and Kataoka, T. (2005) *J. Biol. Chem.* **280,** 31267–31275
19. Ford, B., Skowronek, K., Boykevisch, S., Bar-Sagi, D., and Nassar, N. (2005) *J. Biol. Chem.* **280,** 25697–25705
20. Ford, B., Boykevisch, S., Zhao, C., Kunzelmann, S., Bar-Sagi, D., Herrmann, C., and Nassar, N. (2009) *Biochemistry* **48,** 11449–11457
21. Shima, F., Ijiri, Y., Muraoka, S., Liao, J., Ye, M., Araki, M., Matsumoto, K., Yamamoto, N., Sugimoto, T., Yoshikawa, Y., Kumasaka, T., Yamamoto, M., Tamura, A., and Kataoka, T. (2010) *J. Biol. Chem.* **285,** 22696–22705
22. Spoerner, M., Herrmann, C., Vetter, I. R., Kalbitzer, H. R., and Wittinghofer, A. (2001) *Proc. Natl. Acad. Sci. U.S.A.* **98,** 4944–4949
23. Otwinowski, Z., and Minor, W. (1997) *Methods Enzymol.* **276,** 307–326
24. Leslie, A. G. W. (1992) *Joint CCP4 and ESF-EACBM Newsletter on Protein Crystallography,* No. 26, Daresbury Laboratory, Warrington, UK
25. Collaborative Computational Project Number 4 (1994) *Acta Crystallogr. D* **50,** 760–763
26. Vagin, A., and Teplyakov, A. (1997) *J. Appl. Crystallogr.* **30,** 1022–1025
27. Brünger, A. T., Adams, P. D., Clore, G. M., DeLano, W. L., Gros, P., Grosse-Kunsteleve, R. W., Jiang, J. S., Kuszewski, J., Nilges, M., Pannu, N. S., Read, R. J., Rice, L. M., Simonson, T., and Warren, G. L. (1998) *Acta Crystallogr. D* **54,** 905–921
28. Murshudov, G. N., Vagin, A. A., and Dodson, E. J. (1997) *Acta Crystallogr. D* **53,** 240–255
29. Laskowski, R. A., McArthur, M. W., Moss, D. S., and Thornton, J. M. (1993) *J. Appl. Crystallogr.* **26,** 283–291
30. Spoerner, M., Wittinghofer, A., and Kalbitzer, H. R. (2004) *FEBS Lett.* **578,** 305–310
31. Nicely, N. I., Kosak, J., de Serrano, V., and Mattos, C. (2004) *Structure* **12,** 2025–2036
32. O'Connor, C., and Kovrigin, E. L. (2008) *Biochemistry* **47,** 10244–10246

[4] M. Araki, F. Shima, Y. Yoshikawa, S. Muraoka, Y. Ijiri, Y. Nagahara, T. Shirono, T. Kataoka, and A. Tamura, unpublished results.